Nanocontact Characteristics of Composite Galvanic Chrome Coatings Detected by Sclerometry and Atomic Force Microscopy

Yu.I. Golovin[1,2], V.V. Korenkov[1], S.S. Razlivalova[1], Yu.V. Litovka[3]

[1] *Scientific Research Institute of Nanotechnologies and Nanomaterials,*
G.R. Derzhavin Tambov State University, 33, Internasionalnaya St., Tambov, 392000, Russia;
[2] *Lomonosov Moscow State University, GSP-1, Leninskie Gory, 1, Bld. 11, Moscow, 119991, Russia*
[3] *Tambov State Technical University, 116, Sovetskaya St., Tambov, 392000, Russia*

* Corresponding author: Tel.: 8(4752) 53 26 80. *E-mail*: yugolovin@yandex.ru

Abstract

Using the atomic force microscopy (AFM) and scanning electron microscopy (SEM) the surface morphology of chromium coatings formed from standard electrolytic chromium plating with additional 10–120 mg/l of multi-walled carbon nanotubes (MWCNT) was investigated. Methods of sclerometry (or scratch testing) and AFM were used to study the dependence of the nanocontact characteristics of composite electrochemical chromium coatings on the concentration of CNTs in the electrolyte. With a CNT concentration of 60–70 mg/dm^3 in the electrolyte, the hardness of the Cr/MWCNT coatings increased up to 65 %, the volume of material displaced by scratching decreased to 55 % with respect to pure electrolytic chromium. Improvement of the nanocontact characteristics of composites can be associated with a decrease in the average grain size and a change in the morphology of the coating surface. Using the example of composite chrome coatings, it is shown that the sclerometry method is more sensitive and representative for description of physical-mechanical properties of composite electrolytic coatings, including those with a high surface roughness ($Ra \approx 1.5$–2 μm) than micro- and nanoindentation methods.

Introduction

Understanding regularities and mechanisms of nanocontact deformation of thin films and coatings is necessary for design, development and operation of new structural materials and devices, as well as friction pairs in them [1–3]. The sclerometry method makes it possible to assess physical-mechanical properties of materials and coatings in the nano- and submicrometer range of test depths, and can also be considered as a model of abrasive wear with the closest approximation to the real conditions of interaction in local tribocontacts. This method can be used to study the mechanisms of wear of thin films and coatings [4–6]. The sclerometry method has a number of advantages for the estimation of hardness in the nanoscale with respect to traditional indentation. These advantages include a decreasing impact of surface roughness due to the possibility of averaging the data, reducing the effect

of elastic recovery on the width of scratches [7]. At present, investigation of physical-mechanical properties and deformation processes in submicro- and nano-volumes of composite materials by various methods, such as micro- and nanoindentation, sclerometry, as well as comparing various methods of testing, processing data and choosing among them the most representative is of particular interest [8].

It is known that carbon nanotubes (CNTs) have unique properties, including high mechanical strength and rigidity (the tensile strength σ_y of real nanotubes reaches several tens of GPa, the elastic modulus E is hundreds of GPa), chemical stability, high specific surface area (~ 1000 m^2/g), therefore they are one of the most promising reinforcing elements for metal matrices and coatings [9]. Composites with nanotubes as a reinforcing phase are usually manufactured by methods of thermal spraying, sintering, powder

metallurgy, spark plasma extrusion, and spark plasma sintering. Due to mechanical alloying in the manufacture of the composite, it was possible to achieve a uniform distribution of CNT in the metal matrix [10, 11]. It is known that the degree of uniformity of the CNT distribution in a metal matrix is one of the key factors that affect the resulting physical-mechanical properties of the composite [10]. The formation of a chemical bond between the nanotube and the matrix made it possible to achieve an increase in the compressive yield strength and a decrease in wear resistance by a factor of three, as well as a Vickers hardness growth up to 2 times for Cu-10 % (bulk) CNT composites made by spark plasma sintering [12, 13]. However, to date, the nanocontact physical-mechanical properties of composite materials containing CNTs, including electrolytic coatings, have not been adequately studied. The studies that involved scratch testing were carried out mainly for Al-Si-CNT and Al$_2$O$_3$-CNT alloys obtained by hot pressing [14], cold gas-dynamic spraying [15, 16] and plasma deposition on a substrate [17, 18]. It was found that with a weight content of CNT in an alloy of 1 wt %, the wear resistance of Al-Si-CNT increased by 40 % with respect to Al-Si [16].

Due to excellent performance characteristics, among which high hardness, wear and corrosion resistance, and reflectivity, galvanic chrome coatings have found wide application in various industries such as automotive and aerospace, instrumentation, agriculture, mining and chemical industries [19]. In order to modify the coatings, powders of microparticles of carbides, borides, nitrides (for example, γ-BN) [20], Al$_2$O$_3$, ZrO$_2$, B, Cr$_2$O$_3$, α-C, SiO$_2$ nanoparticles [21- 24], ultradispersed diamonds [25] were added to "trivalent" and "hexavalent" electrolytes. To significantly improve the performance of electrochemical chrome coatings, a high concentration of detonation nanodiamonds or Al$_2$O$_3$ and SiO$_2$ nanoparticles in the chromium electrolyte ($C \sim 10$ g/dm^3) was required [22, 26, 27]. The addition of carbon nanotubes at concentrations of $C = 1$–2 g/dm^3 to electrolytes based on trivalent chromium made it possible to significantly increase the microhardness (by 30-50%) of the chromium coatings [28, 29]. It was shown in [30] that a relatively low concentration of carbon nanotubes in the electrolyte (~ 10 mg/dm^3) also contributes to a noticeable increase in microhardness of electrochemical nickel coatings. Thus, the microhardness of Ni/MWCNT increased by 40 % with the concentration of nanotubes in the nickel plating electrolyte $C = 40$ mg/dm^3 by reducing the average

grain size from 2.2 μm for pure electrolytic nickel to 0.8 μm for the composite [31]. The aim of this work was to investigate the nanocontact propoerties (hardness and volume of the displaced material during scratching) of electrochemical chromium coatings formed from a standard chromate sulphate electrolyte with the addition of MWCNT (from 10 to 120 mg/dm^3) by scratch testing and to compare data obtained by this method and by microindentation.

Materials and methods

Electroplating of chromium-based composite coatings was carried out from a standard sulfate electrolyte widely used in industry containing 250 g/dm^3 of chromic anhydride (CrO$_3$) and 2.5 g/dm^3 of sulfuric acid (H$_2$SO$_4$) at a temperature of $T = 50$ °C. The powdered TAUNIT MWCNTs produced locally at NanoTechCenter, Tambov (Russia) were purified from the catalyst and added to the chrome plating electrolyte. The concentration C of TAUNIT in the electrolyte varied from 10 to 120 mg/dm^3. The MWCNTs were synthesized by catalytic pyrolysis of natural gas on a Ni/Mg catalyst at atmospheric pressure and temperature of 620 °C. The main characteristics of the TAUNIT carbon nanomaterial are given in Table 1. The TEM images of the TAUNIT carbon nanomaterial and an individual multi-walled carbon nanotube characterized by the conical arrangement of graphene layers are shown in Fig. 1 *a* and 1 *b*, respectively.

The laboratory setup for galvanic coating was a 1.5 liter titanium bath equipped with a bubbler placed in a hot water bath to maintain the desired process temperature. The galvanic bath was supplied from stabilized current sources B5-1820 or from the industrial rectifier unit Pulsar Pro 50/12 54.

Table 1

Main properties of the TAUNIT carbon nanomaterial

Outer diameter, nm ………………………....	20–70
Inside diameter, nm ……………………….	5–10
Length, μm ………………………………...	~ 1
Total impurities, % wt	
initial ……………………………………	≤ 5
(after purification) ……………………..	≤ 1
Bulk density, g/cm^3 ……………………….	0.4–0.6
Specific surface area, m^2/g ……………….	120–130
Thermal stability in air, °C ………………...	600

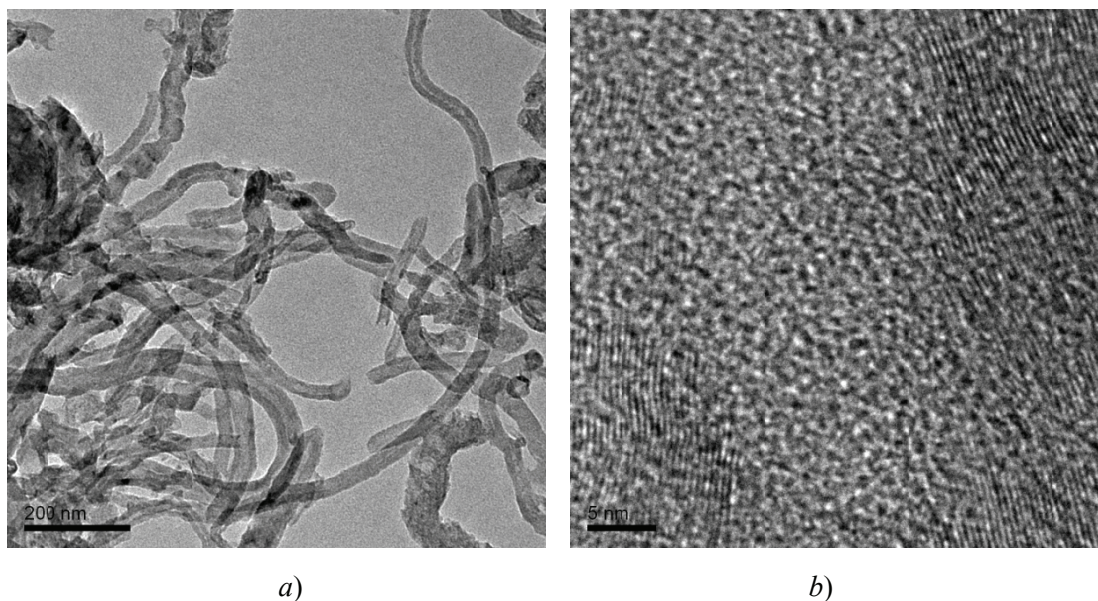*a)*   *b)*

Fig. 1. TEM image of TAUNIT carbon nanomaterial (*a*);
TEM image of the arrangement of graphene layers in a separate multi-walled carbon nanotube (*b*)

The process scheme of chromium electroplating was in compliance with GOST 9.305–84 and comprised the stages of degreasing the surface of steel parts in cold water, washing in cold non-flowing water, etching (50 % HCl solution) for 8–10 min, cold rinse for 2 min, hot flushing in distilled water just before coating.

Square plates made of steel grade St3 with the area of 0.1 dm^2 were used as a cathode, and a plate of the alloy 90 % Pb and 10 % Sn was used as an anode. To achieve the required concentration of Cr^{6+} ions, the electrolyte was run-in at a current density $D_k = 20$ A/dm^2 for 8 hours at $T = 52$ °C. Fig. 2 shows a diagram of the change in the current density over time when chromium was deposited on a steel part. Precipitation of chromium was carried out after heating the parts to the temperature of the electrolyte, the anodic activation, and the current impact necessary for the formation of chromium crystal nuclei. To reduce the size of agglomerates from nanotubes prior to the electrochemical deposition process, the electrolyte was subject to ultrasound treatment in an IL-100-6/4 setup (frequency $f = 22$ kHz). Ultrasound dispersion was carried out at a sound intensity $I = 7.86 \times 10^6$ W/m^2, corresponding to the amplitude of ultrasonic waveguide oscillations of 80 μm.

Evaluation of hardness and wear resistance of chrome coatings was carried out by microhardness measurement and sclerometry methods. The microhardness H_V was measured on a PMT-3M instrument with a load on the Vickers indenter $P = 1.5$ N. Sclerometric tests were carried out at TriboNanoindenter-NANO instrument for measurement of physical-mechanical properties of submicrometer volumes and near-surface layers of solids; the tool was developed at the Research Institute of Nanotechnology and Nanomaterials, G.R. Derzhavin Tambov State University. (Tambov) and had load resolution $\Delta P = 1$ μN and depth resolution $\Delta h = 0.5$ nm. Scratches were applied with a Berkovich diamond indentor in "edgewise" direction with a normal force $P = 200$ mN and the speed of the indenter displacement $V = 25$ μm/s. The length of the individual scratch was $l = 250$ μm.

The surface topography and scratches were analyzed using a high-resolution scanning electron microscope Merlin (Carl Zeiss, Germany) and a scanning probe microscope DiInnova (Veeco, USA) in a semi-contact mode. The surface roughness was evaluated using an optical profilometer Wyko NT 9080 (Bruker AXS, USA). The procedure for measuring
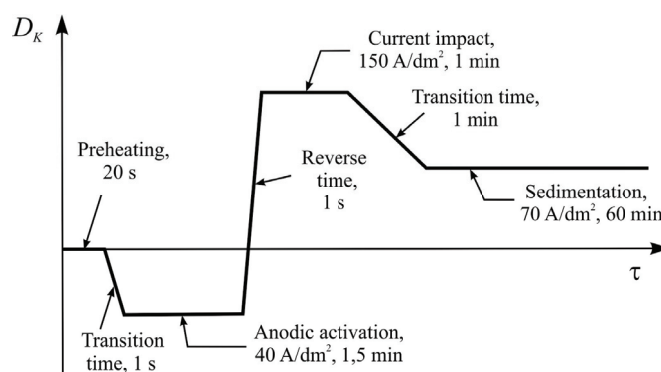

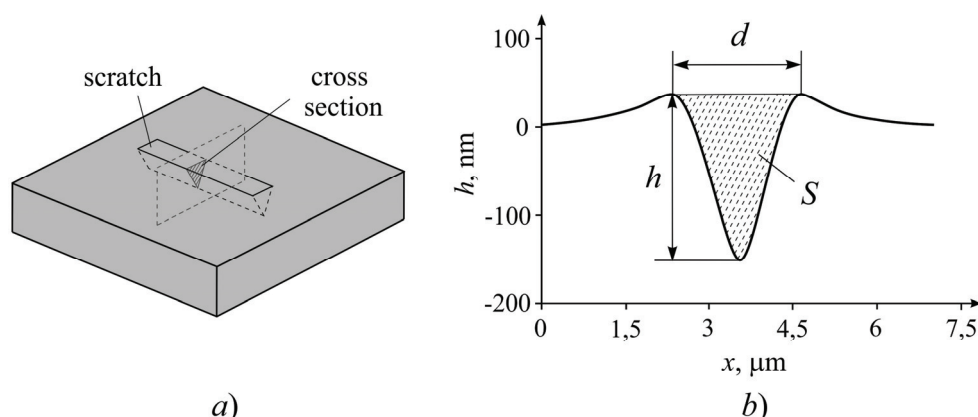**Fig. 2. Diagram of current density variation in time**

Fig. 3. Procedure for measurement of hardness and volume of wear by the sclerometry method:
a – a schematic image of a scratch on the surface of the sample;
b – the principle of measuring the cross-sectional area and the width of the scratch

hardness H_{sc} by sclerometry was based on the analysis of deep scratch profiles according to AFM data. The hardness of coatings was determined by the formula [15]:

$$H_{sc} = k\frac{P}{d^2},\qquad(1)$$

where *P* is normal load [N], *d* is arithmetic mean of the scratch width [m], *k* is coefficient depending on the indenter's shape. To determine the coefficient *k*, scratches were applied to a sample with a known value of microhardness (fused quartz). To calculate the amount of wear, the groove of wear was divided into individual segments with approximately equal cross-sectional areas. The amount of wear was determined by summing the volumes of individual segments of the scratch. Wear volume, normalized to 1 μm wear track (V^*) was determined by the results of at least 65 individual measurements. The area of the scratch section and its width was calculated from the data of the deep surface profiles. The width of the scratches was calculated taking into account the pile up around the scratches. The scheme for measuring the width of the scratch and the cross-sectional area is shown in Fig. 3.

Results and discussion

Using the SEM method, it was found that the structure of the electroplating chrome coatings was typical of a bumpy one with a small number of cracks. Also, carbon nanotubes embedded in a metal matrix were observed on the surface of the coating subjected to local deformation (Fig. 4). From the analysis of AFM images of the surface it follows that the samples obtained at high concentrations of MWCNT in the electrolyte $C = 60–120$ mg/dm³ had a more pronounced surface relief with distinct grain boundaries, with

respect to samples without nanotubes or with low concentrations of them $C = 0$, $C = 10$ mg/dm³, $C = 40$ mg/dm³ (Fig. 5, insert). This observation is confirmed by the construction of surface profiles (Fig. 5), on which rounded protrusions on the surface (individual grains) are clearly visible for samples deposited at $C = 70$ mg/dm³.

Fig. 6 shows the dependence of the roughness index *Ra* (arithmetic mean deviation of the profile from the midline), *Rz* (the height of the unevenness of the profile by ten points) of coatings from the concentration of MWCNT from interferometry data. For pure electrolytic chromium, *Ra* took values of 1.5–2 μm. At $C \leq 30$ mg/dm³, the values of *Ra* and *Rz* did not change significantly. The values of *Ra* and *Rz* had the maximum values (2.2 and 19.6 μm, respectively) for composites deposited at $C = 60$ mg/dm³.

With the growth of *C* in the electrolyte from 0 to 60 mg/dm³, a significant reduction in the average grain size *d* was not observed, which was also characteristic
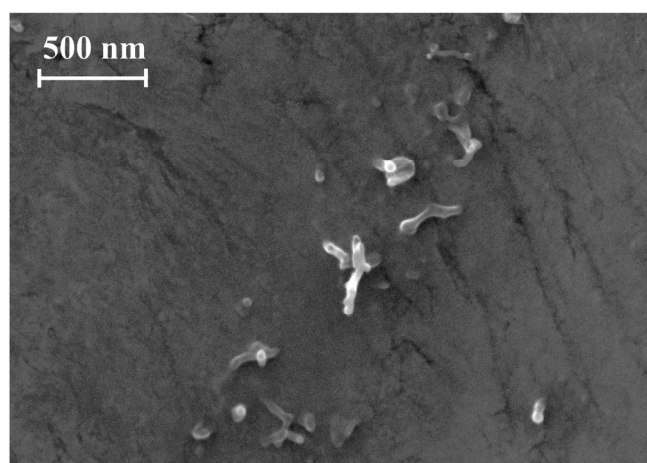

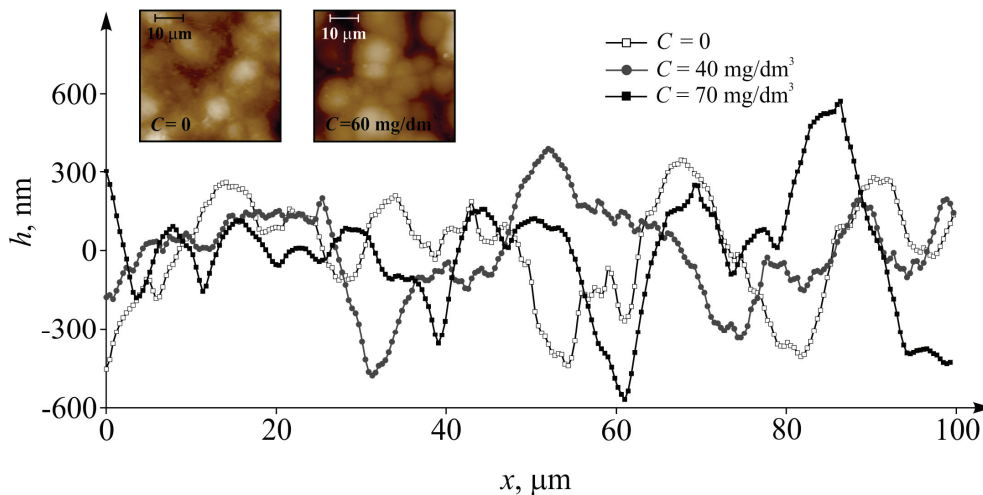**Fig. 4. SEM-image of carbon nanotubes embedded in a metal matrix**

Fig. 5. Surface topography of samples obtained at $C = 0$, $C = 40$ mg/dm^3, $C = 70$ mg/dm^3
(In the inset: AFM-images of coatings deposited at $C = 0$, $C = 60$ mg/dm^3, the scanning region size is 50×50 μm)

of nanocomposite nickel coatings deposited at $C = 40$ mg/dm^3 (d decreased from 2.2 μm to 0.8 μm) [30, 31]. Thus, d was 8–12 μm at $C = 0$ in the electrolyte, $d = 8$–10 μm at $C = 10$ mg/dm^3, $d = 9$–10 μm at $C = 30$ mg/dm^3, $d = 10$–12 μm at $C = 60$ mg/dm^3. A small increase in d at $C = 60$ mg/dm^3 was accompanied with an increase in surface roughness.

For coating deposited at $C = 70$ mg/dm^3, a larger number of fine grains with sizes up to 5 μm were observed (Fig. 7), with d being 7–10 μm. As can be seen from the histogram of grain size distribution, grains larger than 15 μm in the composite were practically not observed, in contrast to pure chromium. It is probably evidence that the ends of nanotubes and defects on their surface could serve as precursors for the nucleation and growth of new grains.

The correlation between the nanocontact characteristics H_{sc} and V^* of chromium coatings and the MWCNT concentration in the electrolyte were investigated by scratch testing at a normal load $P = 200$ mN. The Cr/MWCNT composites exhibited a significant improvement in nanocontact characteristics with respect to chromium deposits not containing CNTs.

At $C = 70$ mg/dm^3, the average hardness value was $H_{sc} = 12.3$ GPa, which was 65 % higher than the hardness of pure chromium control coatings ($H_{sc} \approx 7.5$ GPa) (Fig. 8), with the scratch width decreasing from 8.5–9 to 5–7 μm (Fig. 9).

It was established in [32] that the average values H_V of chromium coatings ranged from 8.8 to 11.3 GPa, depending on the weight content of CNTs in the electrolyte (Fig. 8). At $C = 60$ mg/dm^3, the electrolytic
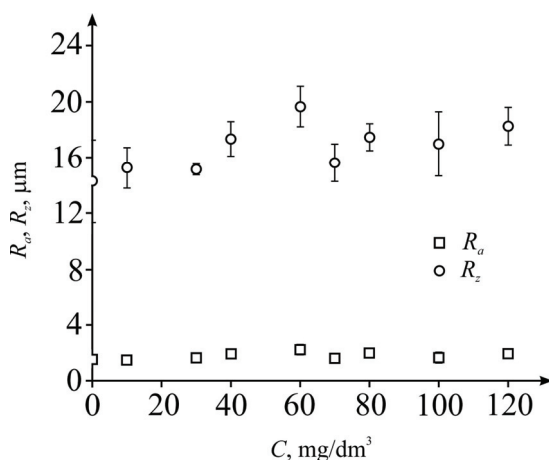

Fig. 6. Correlation between the coating roughness and the CNT concentration in the electrolyte of chrome plating

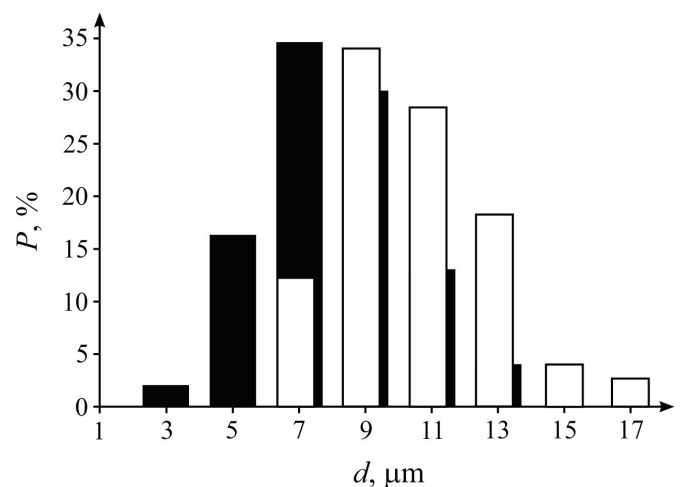**Fig. 7. Graphs of grain size distribution for coatings deposited at $C = 70$ mg/dm^3 (black bars) and at $C = 0$ (white bars)**

chrome coating had the highest microhardness index $H_V = 11.3$ GPa, which was 28 % higher than the hardness of the coating without CNTs (8.8 GPa). It should be noted that the $H_{sc}(C)$ dependence was qualitatively correlated with the behavior of the microhardness $H_V(C)$ of coatings. This fact can be explained by similarity of deformation mechanisms acting for submicro- and micrometer volumes of locally deformed material. Hence, both methods are applicable for studying the physical-mechanical properties of composite electrolytic coatings, but the sclerometry method is more adequate to the real wear conditions and records a greater increase in wear resistance.

The volume of the displaced material was calculated from the depth profiles of scratches acquired using AFM. The dependence of the averaged values of
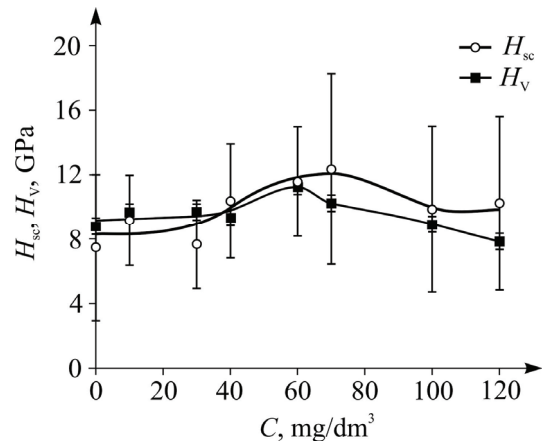

Fig. 8. Correlation between hardness determined in the present work by the sclerometry method, and Vickers's microhardness of chromium coatings from the concentration of nanotubes in the electrolyte (adapted from [32])
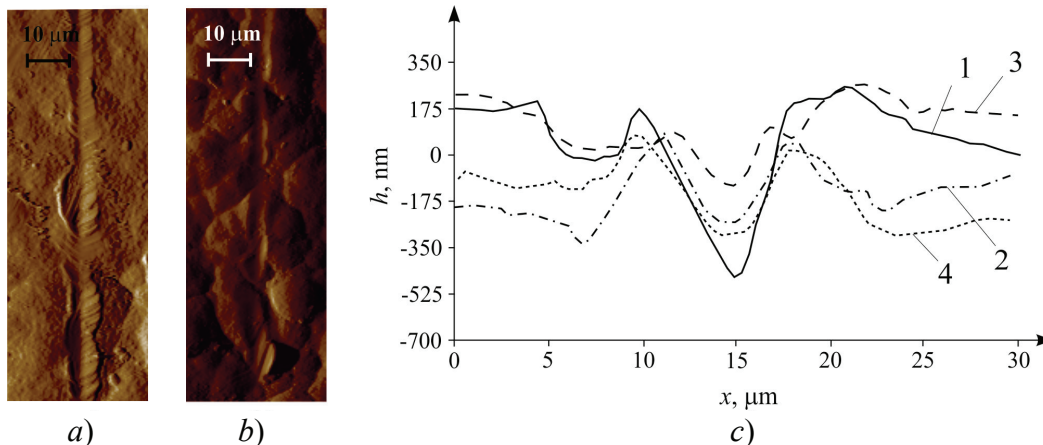

a)   *b)*   *c)*

Fig. 9. Typical AFM images of scratches on the coatings formed at $C = 0$ (*a*) and $C = 70$ mg/dm^3 (*b*) and scratch depth profiles (*c*) for $C = 0$ (*1*), $C = 60$ mg/dm^3 (*2*), $C = 70$ mg/dm^3 (*3*), $C = 120$ mg/dm^3 (*4*)
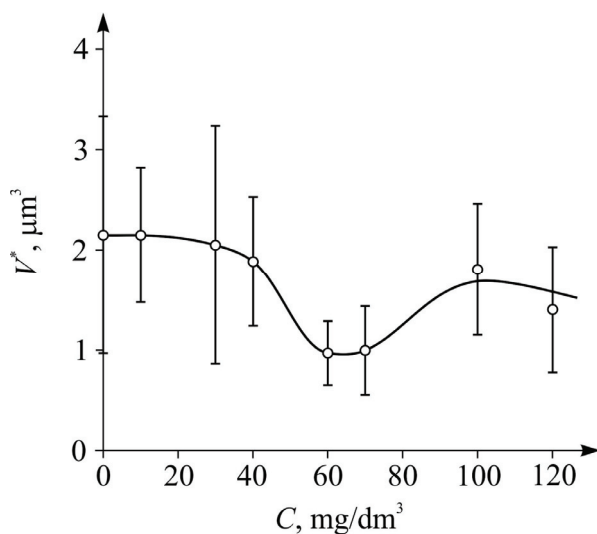

Fig. 10. Correlation between the wear volume V^* given on 1 μm of the wear track and the CNT concentration in the precipitating bath

V^* on the CNT concentration is shown in Fig. 10. As can be seen from the Fig. 10, at $C = 70$ mg/dm^3, V^* decreased to 55 %. Because of the strong effect of elastic recovery on the residual depth of scratch, V^* of coatings obtained at $C = 100$ mg/dm^3 and $C = 120$ mg/dm^3 were slightly lower than in pure chromium, but nanohardness growth was not observed due to insignificant effect of elastic recovery on the width of scratches. As can be seen from the Figure, the dependences of V^* on the nanotube concentration correlated with the behavior of $H_{sc}(C)$ and $H_V(C)$.

It is known that the main factors affecting the microhardness of electrolytic chromium are the presence of hydrogen and oxygen in the deposits, internal stresses, grain size [33]. Hydrogen is adsorbed by chromium and is located along the grain boundaries, in microcracks, in the crystal lattice of the metal. The introduction of nanotubes into a metal matrix can

reduce the impact of hydrogen on crystallization processes. The maximum hardness values and the largest reduction in the volume of the displaced material were achieved for coatings deposited at $C \geq 70$ mg/dm^3 due to a decrease in the average grain size.

Thus, the sclerometry method is more relevant for studying the physical-mechanical properties of composite electrolytic coatings, including those with a high surface roughness ($Ra \approx 1.5$–2 μm) than measuring micro- and nano-hardness. This test method is most preferable for measurement of physical and mechanical properties of composite coatings compared to other tests (indentation methods) due to higher information capacity and accuracy resulting from the opportunity of data averaging and reduced impact of elastic recovery [6].

Conclusion

1. A method of scratch testing with low load (200 mN) was used to investigate the correlation between the nanocontact characteristics of composite chromium coatings and the concentration of multi-walled carbon nanotubes in the chromium electrolyte. The Cr-MWCNT composites formed from a standard chromium electrolyte with the addition of MWCNT from 10 to 120 mg/l, demonstrated improved nanocontact characteristics with respect to pure electrolytic chromium. At $C = 70$ mg/dm^3, the hardness H_{sc} increased up to 65 %, the volume of the displaced material V^* decreased to 55 %.

2. The improvement of nanocontact characteristics of the Cr/MWCNT composites can be caused by a decrease in the average grain size and a change in the morphology of the coating surface. Using the example of composite chromium coatings, it was shown that the sclerometry method is more relevant for description of tribological properties of composite electrolytic coatings, including those with a high surface roughness ($Ra \approx 1.5$–2 μm) than micro- and nanoindentation.

References

1. Nanotribology and Nanomechanics: An Introduction (2nd edition). (ed. B. Bhushan). Springer-Verlag. Berlin, Heidelberg. 2008. 1516 p.

2. Handbook of Nanotechnology. (Ed. B. Bhushan). Springer-Verlag. Berlin, Heidelberg. 2010. 1964 p.

3. Golovin Yu.I. *Vvedenie v nanotekhniku* [Introduction to nanotechnology]. Moskva, Mashinostroenie, 2007, 496 p. (Rus)

4. Golovin Yu.I. *Osnovy nanotekhnologij* [Fundamentals of Nanotechnology]. Moskva, Mashinostroenie, 2012, 656 p. (Rus)

5. Golovin Yu.I. *Nanoindentirovanie i ego vozmozhnosti* [Nanoindentation and its capabilities]. Moskva, Mashinostroenie, 2009. 312 p. (Rus)

6. Shugurov A.R, Panin A.V., Shesterikov E.V. Sclerometric study of galvanic AuNi and AuCo coatings. *Technical Physics Letters*, 2011, vol. 37, issue 3, pp. 223-225.

7. Useinov S.S., Solov'ev V.V., Gogolinskij K.V., Useinov A.S., L'vova N.A. Izmerenie mekhanicheskih svojstv materialov s nanometrovym prostranstvennym razresheniem [Measurement of mechanical properties of materials with nanometer spatial resolution]. *Nanoindustriya* [Nanoindustry], 2010, issue 2, pp. 30-35. (Rus)

8. Golovin Yu.I. Nanoindentation and mechanical properties of solids in submicrovolumes, thin near-surface layers, and films: A review. *Physics of the Solid State*, 2008, vol. 50, issue 12, pp. 2205-2236.

9. Kang I., Heung Y. Y., Kim J.H., Lee J.W., Gollapudi R. Introduction to carbon nanotube and nanofiber smart materials. *Composites: Part B*, 2006, vol. 37, pp. 382–394.

10. Chandran P., Sirimuvva T., Nayan N., Shukla A.K., Murty S.V.S.N., Pramod S.L., Sharma S.C., Bakshi S.R. Effect of carbon nanotube dispersion on mechanical properties of aluminum-silicon alloy matrix composites. *J. Mat. Eng. Perf,*. 2014, vol. 23, issue 3. pp. 1028-1037.

11. Manikandan P., Sieh R., Elayaperumal A., Le H.R., Basu S. Micro/nanostructure and tribological characteristics of pressureless sintered carbon nanotubes reinforced aluminium matrix composites. *Journal of nanomaterials*, 2016, vol. 2, pp. 1-10.

12. Cha S.I., Kim K.T., Arshad S.N., Mo C.B., Hong S.H. Extraordinary strengthening effect of carbon nanotubes in metal-matrix nanocomposites processed by molecular-level mixing. *Adv. Mater.*, 2005, vol. 17, issue 11, pp. 1377-1381.

13. Kim K.T., Cha S.I., Hong S.H. Hardness and wear resistance of carbon nanotube reinforced Cu matrix composites. *Mat. Sci. Eng. A*, 2007, vol. 449-451, pp. 46-50.

14. Chandran P., Sirimuvva T., Nayan N., Shukla A.K., Murty S.V.S.N., Pramod S.L., Sharma S.C., Bakshi S.R. Effect of carbon nanotube dispersion on mechanical properties of aluminum-silicon alloy matrix composites. *J. Mat. Eng. Perf.*, 2014, vol. 23, issue 3, pp. 1028-1037.

15. Bakshi S.R., Singh V., Balani K., McCartney D.G., Seal S., Agarwal A. Carbon nanotube reinforced

aluminum composite coating via cold spraying. *Surf. Coat. Tech.*, 2008, vol. 202, issue 21, pp. 5162-5169.

16. Chen Y., Bakshi S.R., Agarwal A. Correlation between nanoindentation and nanoscratch properties of carbon nanotube reinforced aluminum composite coatings. *Surf. Coat. Tech.*, 2010, vol. 204, issue 16-17, pp. 2709-2715.

17. Bakshi S.R., Lahiri D., Patel R.R., Agarwal A. Nanoscratch behavior of carbon nanotube reinforced aluminum coatings. *Thin Solid Films*, 2010, vol. 518, issue 6, pp. 1703-1711.

18. Balani K., Harimkar S.P., Keshri A., Chen Y., Dahotre N.B., Agarwal A. Multiscale wear of plasma-sprayed carbon-nanotube-reinforced aluminum oxide nanocomposite coating. *Acta Mater.*, 2008, vol. 56, pp. 5984-5994.

19. Lausmann G.A. Current industrial practices Electrolytically deposited hardchrome. *Surf. Coat. Techn.*, 1996, vol. 86-87, pp. 814-820.

20. Gadalov V.N., Serebrovskij V.V., Shcheren-kova I.S., Abakumov A.V., Turaeva O.A. Struktura i svojstva ehlektroliticheskih hromovyh pokrytij s ul'tradispersnym sverhtverdym napolnitelem [Structure and properties of electrolytic chrome coatings with ultradisperse superhard filler]. *Vestnik MGTU im. G.I. Nosova*, 2012, vol. 14, pp. 39-45. (Rus)

21. Tseluikin V.N. Composite coatings modified with nanoparticles: structure and properties. *Nanotechnologies in Russia*, 2014, vol. 9, issue 1-2, pp. 1-14.

22. Vodop'yanova S.V., Fomina R.E., Mingazo-va G.G. EHkspluatacionnye harakteristiki hromovyh pokrytij s dispersnoj fazoj nanoporoshka oksida alyuminiya [Performance characteristics of chrome coatings with a dispersed phase of nanopowder alumina]. *Vestnik kazanskogo tekhnologicheskogo universiteta*, 2011, issue 12, pp. 144-150. (Rus)

23. Sajfullin R.S., Hacrinov A.I., Vodop'ya-nova S.V., Mingazova G.G., Fomina R.E. Issledovaniya v oblasti sozdaniya kompozicionnyh ehlektrohimicheskih pokrytij (KEHP) s dispersnoj fazoj mikro- i nanochastic [Research in the field of creating composite electrochemical coatings (CEC) with a dispersed phase of micro- and nanoparticles]. *Vestnik kazanskogo tekhnologicheskogo universiteta*, 2009, issue 6, pp. 80-90. (Rus)

24. Salahova R.K., Semenychev V.V., Il'in V.A. Vliyanie processa «trekhvaletnogo» hromirovaniya konstrukcionnoj stali na ee ehkspluatacionnye harakteristiki [The effect of the process of "three-graded" chromium plating of structural steel on its performance characteristics]. *Vestnik Samarskogo universiteta*. 2011, issue 3-1, pp. 287-293. (Rus)

25. Burkat G.K., Dolmatov V.Yu. Application of ultrafine-dispersed diamonds in electroplating. *Physics of the Solid State*, 2004, vol. 46, issue 4, pp. 703-710.

26. Burkat G.K., Dolmatov V.Yu., Osawa E., Orlova E.A. A study of properties of chromium-diamond coatings using nanodiamonds from various producers, *Journal of Superhard Materials*, 2010, vol. 32, issue 2, pp. 98-111.

27. Vodop'yanova S.V., Mingazova G.G., Fo-mina R.E., Sajfullin R.S. Issledovanie vliyaniya nanochastic SiO2 na ehlektroosazhdenie hromovyh pokrytij i ih svojstva [Investigation of the influence of SiO2 nanoparticles on electrodeposition of chromium coatings and their properties]. *Vestnik kazanskogo tekhnologicheskogo universiteta*, 2012, issue 15, pp. 77-80. (Rus)

28. Maharaja J., Raja M., Mohan S. Pulse electrodeposition of Cr-SWCNT composite from choline chloride based electrolyte. *Surf. Eng.*, 2014, vol. 30, issue 10, pp. 722-727.

29. Liu, B., Zeng Z., Lin Y. Mechanical properties of hard Cr-MWNT composite coatings. *Surf. Coat. Techn.*, 2009, vol. 203, issue 23, pp. 3610–3613.

30. Golovin Yu.I., Litovka Yu.V., Shuklinov A.V., Vasyukov V.M., Stolyarov R.A. Nickel galvano-chemical coating modified by carbon nanotubes. *Russian Metallurgy*, 2012, issue 4, pp. 336-338.

31. Stolyarov R.A. *Poluchenie, struktura i svojstva gal'vanicheskih pokrytij (Ni) i ob"emnyh materialov (Ni, Ag), modificirovannyh uglerodnymi nanotrubkami. Diss. kand. tekhn. nauk* [The preparation, structure and properties of galvanic coatings (Ni) and bulk materials (Ni, Ag) modified with carbon nanotubes. Diss. Cand. tech. sci.]. Tambov, 2016, 109 p. (Rus)

32. D'yakov I.A. *Nauchnye i tekhnologicheskie osnovy polucheniya nanostrukturnyh gal'vanicheskih pokrytij. Dokt. Diss* [Scientific and technological basis for obtaining nanostructured galvanic coatings. Doct. diss]. Tambov, 2017, 334 p. (Rus)

33. Brenner A., Burkhead P., Jennings C. Physical properties of electrodeposited chromium. *Journal of Research of the National Bureau of standards*. 1948, vol. 40, pp. 31-59.